AIAA 81-1522R

Rotating Valve for Velocity-Coupled Combustion Response Measurements

R.S. Brown,* R.C. Waugh,† and V.L. Kelly‡
United Technologies, Sunnyvale, Calif.

A dual rotating valve apparatus has been investigated for measuring the velocity-coupled response function of solid propellants. Bulk mode velocity oscillations are generated by operating rotating valves 180 deg out of phase at each end of a combustion chamber. Analytical studies were conducted using both a linear and a nonlinear velocity-coupling model to demonstrate feasibility and to develop data reduction methods. A method for extracting the linear response from oscillatory pressure measurements was demonstrated. No satisfactory method was found for deriving both the nonlinear response parameter and the threshold velocity. Coldflow tests validated the apparatus performance. Combustion tests provided linear velocity-coupled response functions for two nonaluminized and one aluminized propellants at frequencies between 150 and 600 Hz. Reasonable reproducibility was demonstrated and response values compared favorably to previously reported test-burner results. Spectral analysis of the oscillatory pressure indicates, however, a nonlinear velocity-coupling model may provide a more realistic interpretation of the response.

Nomenclature

a = sonic velocity
A = acoustic admittance
arg( ) = phase angle
C = constant in Eq. (3)
d = diameter
D,E = integration constants in Eq. (4)
f = frequency
F = particle damping term
$h( )$ = Heaviside unit step function
i = $\sqrt{-1}$
Im( ) = imaginary part of ( )
k = constant in Eq. (3)
K = Kummer's function
L = chamber length
M = Mach number
M^* = definition in Eq. (9)
N = constant in Eq. (3)
p = pressure
q = chamber pressure
r = transformed length (also burn rate in Figs. 9-11)
R = response function
Re( ) = real part of ( )
S = area
t = time
T = temperatures
T_k = $i\lambda - A_b qL/S$
Z = dimensionless chamber length
α = exponential growth rate
γ = specific heat ratio
$\hat{\epsilon}$ = acoustic pressure = $\hat{p}/\gamma\bar{p}$
λ = dimensionless frequency = $2\pi fL/a$
$\hat{\mu}_1$ = fundamental component in Fourier decomposition of nonlinear velocity coupling at the driving frequency
$\hat{\sigma}$ = flow turning parameter = $\hat{M}(d\bar{M}/dZ)$
$\overline{x_1}$ = value of Z at which $\bar{M}=0$ and is given by $\bar{S}_{v_0}/(\bar{S}_{v_0}+\bar{S}_{v_1})$
$\hat{\psi}$ = dimensionless area = $\bar{S}/\bar{S}$
ω = response of flame temperature

Subscripts and Superscripts

b = burning surface
c = chamber
f = flame
p = pressure coupling
th = threshold
v = velocity coupling
0 = at $Z=0$
1 = at $Z=1$ (also component of Fourier decomposition of driver frequency)
$\bar{(\ )}$ = time average
$\hat{(\ )}$ = complex amplitude

Introduction

THE stability of the pressure in a solid rocket motor is determined by a delicate balance between the sources and losses in oscillatory energy. The flow characteristics of the nozzle, particle drag, and vibration characteristics of the case and grain are the principal loss mechanisms. The primary sources of energy gain are the flowfield in the motor port and the dynamic combustion properties of the propellant. These properties include the response of the rate of combustion energy release to both acoustic pressure and acoustic velocity oscillations.

While several attempts have been made to predict these responses,[1-5] no adequate prediction methods have been developed to date. Hence emphasis has been placed on measuring these properties in laboratory burners. Both the T-burner[6] and the rotating valve[7,8] are currently being used routinely to measure the response to acoustic pressures.

Measuring the response to acoustic velocities has proven more difficult. Significant effort has been directed to adapting the T-burner for these measurements.[9-11] Unfortunately, significant contributions from the pressure coupling also occur under conditions that maximize the velocity-coupled contributions. Thus independent measurements of the pressure response are required before velocity responses can be determined. More importantly, the uncertainties in the pressure response add to the data uncertainties to increase the error band in the velocity response. There are also additional difficulties resulting from the

Presented as Paper 81-1522 at the AIAA/SAE/ASME 17th Joint Propulsion Conference, Colorado Springs, Colo., July 27-29, 1981; submitted Aug. 12, 1981; revision received Feb. 5, 1982. This paper is declared a work of the U.S. Government and therefore is in the public domain.

*Senior Staff Scientist, Chemical Systems Division. Associate Fellow AIAA.
†Senior Research Engineer, Chemical Systems Division.
‡Associate Research Engineer, Chemical Systems Division.

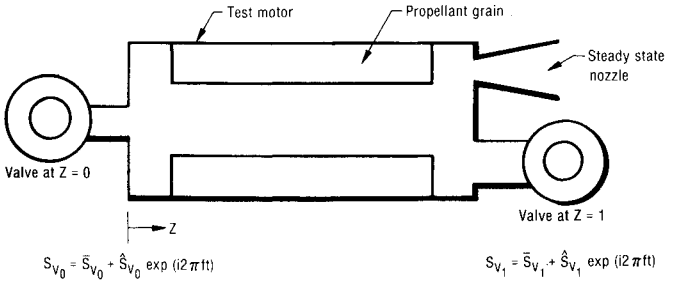

Fig. 1 Schematic of dual rotating valve.

harmonic content in the data[10] and the realism with which the environment in the T-burner represents that in the motor.[11]

Description of Dual Rotating Valve Method

The studies reported here were initiated to explore the dual rotating valve as an alternative method for making velocity response measurements. The dual rotating valve has identical valves at each end of a test burner, as shown in Fig. 1. One or more conventional nozzles are used to control the steady-state pressure. A central feature of the method is the control of the phase between the sinusoidal area oscillations of the two valves. If the two valves are in phase, the oscillating components of area add, and pressure oscillations are driven in the burner. If the valves are 180 deg out of phase, velocity oscillations are produced as the venting of combustion gases alternates between the ends of the burner. Any oscillations in the rate of chemical energy release produced by these oscillations will generate pressure oscillations because the instantaneous total nozzle area is constant. These pressure oscillations can be measured and the velocity response derived using an acoustic analysis of the burner.

This method represents an extension of an approach suggested several years ago by Eisel and co-workers.[12] Their objective was to observe the luminosity response of aluminized propellants to velocity oscillations. Their experiment incorporated two identical choppers for modulating the exhaust flow. They did not, however, include additional conventional nozzles for independently controlling the mean flow environment, nor did they attempt to measure and interpret the pressure oscillations quantitatively.

This method offers several potential improvements over the T-burner. First, when operated at low frequencies (compared to the acoustic modes of the burner), behavior is dominated by velocity-coupling effects, with pressure coupling and particle damping reduced to a secondary role. Second, the velocity response can be measured under different mean flow environments by changing the steady-state nozzles at each end of the burner. Third, there are significant savings in the quantity of propellant and number of tests required to characterize a propellant, compared to the T-burner.

Analytical Studies

Theoretical analyses of the dual rotating valve burner were conducted for two purposes: to determine if accurate measurements of the velocity response can be made, and to calculate the velocity response function from the measured pressure oscillations. This requires two formulations of the basic equations. These analyses are further complicated since two models, one linear and one nonlinear, have been proposed to describe velocity coupling.[13-15] In the linear model, the response depends on the direction of the mean gas flow as well as the magnitude and direction of the oscillating velocity, but does not depend on the magnitude of the mean speed. This model has been used extensively to interpret velocity-coupled T-burner data,[9,10] motor data,[16] and in predictions of motor stability.[17]

The nonlinear model evolved by analogy to erosive burning. In erosive burning, analytical studies[18] and experimental results[19] suggest there is a minimum, or threshold, speed that must be exceeded before the effect of parallel gas flow on the burning rate becomes significant. Extrapolating the threshold speed concept to oscillatory flows is a central feature of the nonlinear response model. The basic hypothesis assumes the burning rate responds to velocity oscillations when the instantaneous total velocity (mean velocity plus the oscillating velocity) exceeds the threshold speed. An analytical formulation of this model was also included in the Standard Stability Prediction Program,[20] but this model has never been adequately verified experimentally.

The basic analysis starts with the one-dimensional equations of motion for the gas in the combustion chamber.[21] After linearizing, nondimensionalizing, dropping terms of $0(\bar{M}^2)$, and assuming sinusoidal oscillations, the momentum and energy equations can be written:

$$i\lambda\hat{M} + \frac{d\hat{\epsilon}}{dZ} + \frac{d(\bar{M}\hat{M})}{dZ} + \hat{\sigma} - \hat{F} = 0 \tag{1}$$

$$i\lambda\hat{\epsilon} + \gamma\frac{d\bar{M}}{dZ}\hat{\epsilon} + \frac{d\hat{M}}{dZ} + \bar{M}\frac{d\hat{\epsilon}}{dZ} = \frac{d\bar{M}}{dZ}[(R_p + \omega_p)\gamma\hat{\epsilon} + (R_v + \omega_v)\hat{\mu}_1] \tag{2}$$

The perturbation in the combustion energy is assumed to depend on acoustic pressure and velocity in Eq. (2). The pressure dependence is straightforward but the form of the velocity dependence is more complex. The linear velocity coupling model assumes that

$$\hat{\mu}_1 = \hat{M} \cdot \bar{M} / |\bar{M}|$$

In the nonlinear velocity-coupling model, $\hat{\mu}_1$ is the fundamental harmonic component of the oscillation in effective gas speed. The details of the evaluation of $\hat{\mu}_1$ are covered in a later section.

Equations (1) and (2) can be combined in the following form:

$$\frac{d^2\hat{\epsilon}}{dZ^2} - 2(CZ - N)\frac{d\hat{\epsilon}}{dZ} - 4Ck\hat{\epsilon} = 0 \tag{3}$$

Equation (3) can be transformed to a Kummer's equation,[22,23] which has the solution

$$\hat{\epsilon} = DK\{k, 1/2, r\} + Er^{1/2}K\{k + 1/2, 3/2, r\} \tag{4}$$

Each end of the combustion chamber is terminated by a sonic nozzle with an oscillating throat area. If quasisteady behavior is assumed, then velocity, temperature, and throat area oscillations at the nozzles can be related by

$$\hat{M} = \bar{M}[\hat{\psi} + 0.5(\hat{T}/\bar{T})] \tag{5}$$

At this point, there is a dilemma in relating the nozzle equation for the oscillating Mach number at each end of the burner to the values derived from Eq. (4). The nozzle equations relate velocity and temperature, while the chamber solution relates velocity to pressure. If the flame temperature oscillations were known separately from the burning rate oscillation, an equation for the entropy oscillation at the nozzle could be derived. Without this knowledge, however, an assumption is required. Traditionally, but without justification, the entropy oscillation at the nozzle entrance is assumed to be zero. The nozzle boundary condition then becomes

$$\hat{M} = \bar{M}[0.5\hat{\epsilon}(\gamma - 1) + \hat{\psi}] \tag{6}$$

There are several significant features of the solution. First, momentum and energy effects are included along with the

transient mass balance contributions. Second, the analysis includes all the stability elements incorporated in the Standard Stability Prediction Model. Third, the analysis permits the study of the two-valve configuration as well as the one-valve configuration. Fourth, the analysis is not restricted to low frequencies. Thus Eq. (4) is a general solution that should be valid for one-dimensional burners at all frequencies.

Solution for Pressure Oscillations for Known Linear Velocity Response

In the linear velocity-coupling model, the burn rate depends on the direction of the mean flow but not on its magnitude. If the mean flow is positive, a positive velocity perturbation produces a positive speed perturbation so the oscillation in velocity and speed are in phase. However, if the mean flow is negative, a positive velocity perturbation produces a negative speed perturbation so the oscillation in the velocity and speed are out of phase. This explains the factor $\bar{M}/|\bar{M}|$ used in the expression for $\hat{\mu}_1$ for linear velocity coupling. Because $\bar{M}/|\bar{M}|$ changes sign when the mean flow Mach number goes to zero, two sets of constants are required in Eq. (4): one set for $\bar{M}/|\bar{M}|<0$ and one for $\bar{M}/|\bar{M}|>0$. The additional boundary conditions are obtained by requiring the oscillatory pressure and velocity to be continuous at the transition point.

Verification of Solution

The solution of the equations described in the preceding paragraphs was verified in three ways. First, at low frequencies, the Kummer's functions in Eq. (4) approach unity. With this simplification, Eq. (4) leads to the equations derived for the pressure-coupled rotating valve.[7,8] Numerical calculations also yield identical results. This is an important point since it provides a numerical verification of the computer programming in addition to the analytical verification. Second, Micci[24] has recently reported the results of numerical integrations of Eqs. (1) and (2). Comparisons between Micci's results and the Kummer's solution show excellent agreement. Hence the solution is not limited to the low-frequency conditions of the rotating valve, but is also applicable to the higher-frequency conditions near the acoustical mode frequencies.

Third, when driving at frequencies near the acoustic modes, one would expect the frequency difference at the half-power amplitudes (i.e., $0.707\times$the peak amplitudes) would be related to the overall system damping of the self-excited system by the expression

$$\alpha/f=\pi\Delta f/f \tag{7}$$

The left side can be evaluated independently from Culick's solutions,[21] while the right side can be evaluated from numerical solutions of Eq. (4). The excellent agreement found for the three cases examined is shown in Table 1. The first case contained only pressure-coupling effects and used one valve. The second and third cases incorporated both pressure and velocity coupling, as well as particle damping effects. In case two, the response functions were low (i.e., 0.2), while in case three, they were approximately an order of magnitude higher.

Deviations of Linear Response from Pressure Oscillation Measurements

In combustion tests, oscillation pressures will be measured and a procedure is needed to derive the responses from measured pressures. Efforts to obtain analytical solutions were not successful. Since the responses are implicit in Eq. (4), rearranging the forward solution to obtain expressions that are explicit in the response was also unsuccessful.

Numerical analyses examined the axial variations in the predicted pressure and velocity oscillations. The pressure and velocity response functions were estimated using the thermal wave combustion model.[1-5,13-15] When the valves are 180 deg out of phase, these calculations show the oscillating velocity is essentially spatially uniform at low frequencies (i.e., $\lambda<0.75$). In addition, the oscillating pressure is shown to be nearly a linear function of axial position. Using this linear pressure observation, an approximate solution of the energy equation can be developed which is explicit in the velocity response:

$$R_v+\omega_v=\left[T_k\hat{\epsilon}_0+\left(2T_k+\frac{d\bar{M}}{dZ}\right)\overline{\chi_1}(\hat{\epsilon}_1-\hat{\epsilon}_0)+(\hat{M}_1-\hat{M}_0)\right]\Big/\left[\left(\frac{d\bar{M}}{dZ}\right)\hat{M}_1(1-2\overline{\chi_1})\right] \tag{8}$$

The maximum error found using Eq. (8) was 10%. This is considered acceptable when compared to the scatter generally obtained in propellant response measurements.

Solution for Nonlinear Velocity Coupling

The nonlinear velocity-coupling model used in this analysis combines kinematic concepts from steady-state erosive burning with a frequency-dependent response function. This model has been studied by Price,[13,14] Culick,[15] and Condon,[5] and was developed by heuristic arguments to qualitatively explain some observed instabilities. Velocity oscillations generate an oscillatory heat flux to the burning propellant surface. The flux is rectified since it depends on the magnitude of the velocity and not the direction. A threshold speed is then added, thereby requiring the instantaneous speed to exceed this threshold before oscillatory effects are produced in the burning rate. The "effective" velocity (i.e., the heat flux) can be expressed as $M^*h(M^*)$, where

$$M^*+|\bar{M}+\mathrm{Re}(\hat{M}e^{i2\pi ft})|-M_{th} \tag{9}$$

The driving parameter for nonlinear velocity coupling $\hat{\mu}_1$ is the fundamental component of the Fourier decomposition of $M^*h(M^*)$. The mathematical details of this decomposition are presented in Brown and Waugh.[25]

Figure 2 shows that $\hat{\mu}_1$ varies almost linearly with $\bar{M}$ for a constant amplitude of the driving velocity oscillation. The

Table 1 Computed system damping (α/f)

Case	Culick analysis	Kummer's equation
1	0.112	0.117
2	0.155	0.156
3	0.102	0.108

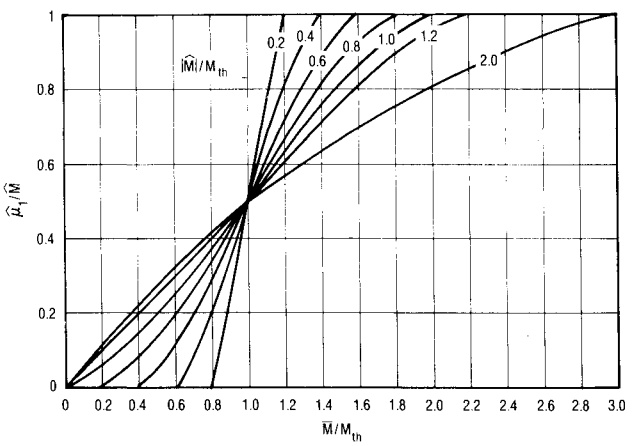

Fig. 2 Fundamental component of "effective" velocity.

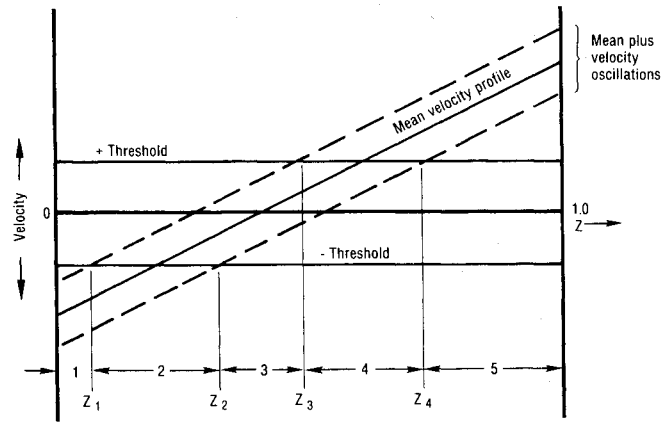

Fig. 3 Description of regions containing nonlinear velocity coupling.

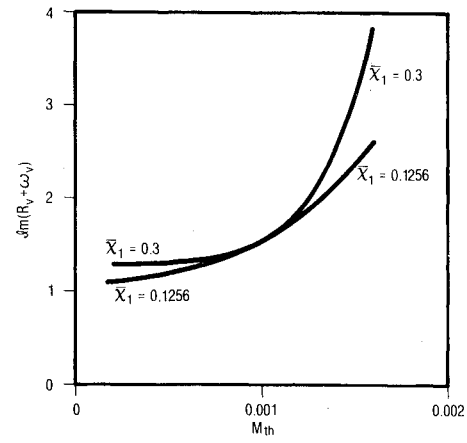

Fig. 4 Plot of $\mathrm{Im}(R_v+\omega_v)$ vs M_{th} for two values of χ_1, (true $M_{th}=0.001$).

parameter $\hat{\mu}_1$ is then combined with a "response function" to produce burning rate (and flame temperature) oscillations according to Eq. (2). A more complete anlaysis of this model can be found in papers by Price and Dehority,[13,14] Culick,[15] and Condon,[5] and in the "Standard Stability Prediction Program Manual."[20]

To apply this model to the chamber requires that the changes in the oscillating velocity, the mean flow velocity, and the threshold velocity all be considered along the length of the chamber. This can best be explained by examining the velocity distributions in the burner, as shown in Fig. 3. The locus of the minimum and maximum values of $M(Z)$ during oscillation are shown dotted above and below $\bar{M}$. Two horizontal lines representing the plus-and-minus thresholds are also shown. The burner is divided into five regions, with each region having a different formulation for the velocity-coupled driving. In regions 1 and 5, linear velocity coupling occurs since $\bar{M}+M'$ is always greater than the threshold value. In regions 2 and 4, nonlinear velocity coupling occurs, while no response is generated in region 3. The linear solutions developed earlier can be used directly in regions 1 and 5. In region 3, the velocity response is zero and the linear equations can then be used directly.

Regions 2 and 4 are more difficult to analyze since both $\hat{M}$ and $\bar{M}$ vary with axial position. One could always resort to numerical integrations; however, Fig. 2 suggests an approximate approach. At low frequencies, $\hat{M}$ is nearly independent of axial position. Since $\bar{M}$ is linear with axial position, this suggests $\hat{\mu}_1/\hat{M}$ is a linear function of axial position in regions 2 and 4. With this approximation, the basic equations can again be transformed into a Kummer's equation by redefining the parameters N and C.[25] Some iteration is required, since the location of the boundaries of regions 2 and 4 depends on $\hat{M}(Z)$. However, the effect is usually small for the low frequencies and the solution converges rapidly.

Solution for Nonlinear Velocity Response from Measured Pressure Oscillations

To derive the nonlinear response from measured pressure oscillations, the energy equation can be written as

$$\frac{d\hat{M}}{dZ} = \left[\frac{d\bar{M}}{dZ}\gamma(R_p+\omega_p) - i\lambda - \gamma\frac{d\bar{M}}{dZ}\right]\hat{\epsilon} - \bar{M}\frac{d\hat{\epsilon}}{dZ} + \frac{d\bar{M}}{dZ}(R_v+\omega_v)\hat{\mu}_1 \tag{10}$$

If $\hat{M}(Z)$ and $\hat{\epsilon}(Z)$ are assumed to vary linearly with axial position, the pressure can be defined in terms of the measured pressures at each end of the burner and the flow oscillation can be derived from the transient nozzle flow equations. Equation (10) can then be integrated to yield

$$\hat{M}(1)-\hat{M}(0) = \int_0^1 \left[\frac{d\bar{M}}{dZ}\gamma(R_p+\omega_p) - i\lambda - \gamma\frac{d\bar{M}}{dZ}\right][\hat{\epsilon}_0+(\hat{\epsilon}_1-\hat{\epsilon}_0)Z]dZ - \int_0^1 \frac{d\bar{M}}{dZ}(Z-\bar{\chi}_1)(\hat{\epsilon}_1-\hat{\epsilon}_0)dZ + \frac{d\bar{M}}{dZ}(R_v+\omega_v)\int_0^1 \hat{\mu}_1 dZ \tag{11}$$

Since $\hat{M}(1)$ and $\hat{M}(0)$ are calculated from the nozzle equation and $\hat{\epsilon}(0)$ and $\hat{\epsilon}(1)$ are measured, the three integrals can be evaluated and a value can be obtained for $(R_v+\omega_v)$. In evaluating the last integral in Eq. (12), the linear relationship between $\hat{\mu}_1$ and $\hat{M}$ is assumed for regions 2 and 4. A finite-difference iterative scheme that relaxes most of the restrictions in this approximate method was also developed.[25]

This method assumes the threshold speed is known. Considerable effort was devoted to the development of a method for deriving this threshold speed from the data, but no direct method could be found. Parametric calculations showed that if several values of M_{th} are used for a given set of $\hat{\epsilon}_0$ and $\hat{\epsilon}_1$, a curve of $\mathrm{Im}(R_v+\omega_v)$ vs M_{th} can be drawn. Figure 4 shows two such curves for different values of χ_1. In the forward solution, each set of $\mathrm{Im}(R_v+\omega_v)$ and M_{th} (for constant $\bar{\chi}_1$) produces $\hat{\epsilon}(0)$ and $\hat{\epsilon}(1)$ values which are nearly identical. Thus there is really no unique solution for M_{th} and $\mathrm{Im}(R_v+\omega_v)$. Qualitatively, this is equivalent to stating that conditions of low response and low threshold speeds cannot be separated from conditions of high response and high threshold speed.

Since the mean flow profile also influences the velocity coupling, calculations were made for two different profiles. Ideally, M_{th} and $\mathrm{Im}(R_v+\omega_v)$ are independent of the mean flow; hence there should be a set of these parameters that are common to both profiles. Unfortunately, Fig. 6 shows that this common set of values will be difficult to determine accurately. Thus separating M_{th} and $\mathrm{Im}(R_v+\omega_v)$ remains an unsolved problem.

Experimental Studies

Apparatus Description

A dual rotating valve apparatus was designed and constructed to test this method for velocity response function measurement. This apparatus, which is shown schematically in Fig. 5, uses many of the design features of the single rotating valve. This arrangement provides the flexibility required to study both velocity and pressure coupling simply by changing the phase between the two rows of holes in the rotor. Significant improvements in materials life were ob-

tained by using 90% tantalum, 10% tungsten in critical stator and rotor components, as suggested by Hewes.[26] Auxiliary coldflow chambers provide a phase reference signal for the area oscillations at each end of the burner.

Kistler pressure transducers monitored the oscillating component of the chamber pressure at each end of the propellant grain and in each of the auxiliary chambers. Taber strain-gage-type transducers monitored the mean pressure in the combustion and the auxiliary chambers. All transducer signals, as well as a timing signal, were recorded on FM tape and played back through appropriate filters and phase meters as described in Refs. 7 and 8.

This arrangement for venting each end of the combustion chamber may compromise the one-dimensional flow behavior. However, design limitations required that either the steady-state nozzles or the oscillating vents be located off the axial centerline since both would not fit. In addition, control of the phasing between the two rotating valves is critical to the success of this experiment. Hence this compromise was accepted as an unfortunate necessity.

Early combustion tests showed that close control of the tolerances on the hole spacing in the valve is essential. Large amplitude modulation in the oscillating pressure was observed in the initial data. Further study showed the modulation frequency occurred every 20 cycles, corresponding to the number of holes around the rotor. New rotor sleeves were made to more exacting tolerances. Results using these new rotors, which are in Fig. 6, show the modulations were essentially eliminated.

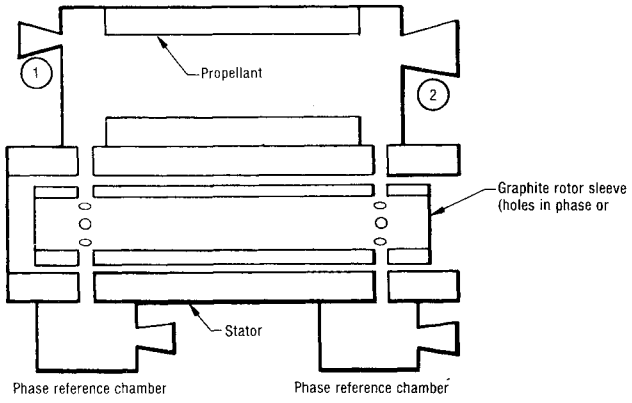

Fig. 5 Apparatus layout.

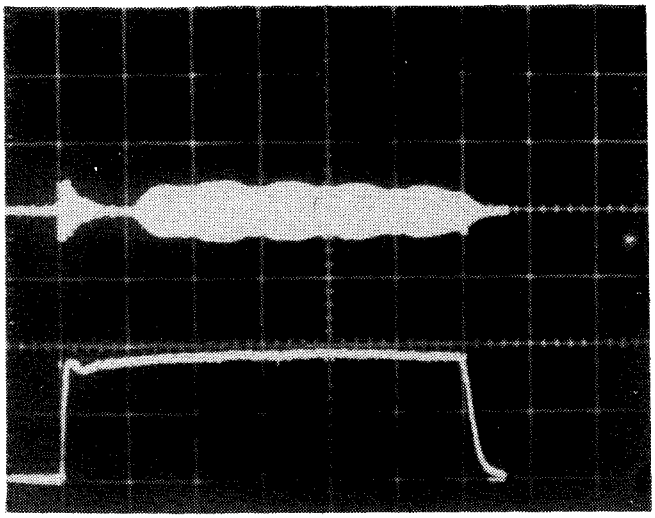

Fig. 6 Data using improved sleeve (test frequency = 150 Hz).

Coldflow Tests

Coldflow tests were conducted as the first step in experimentally evaluating this apparatus. In these studies, nitrogen was injected into the combustion chamber and the two auxiliary chambers through individual sonic chokes. The discharge coefficients of all three exhaust nozzles were evaluated by calibration against a standard Venturi flowmeter. Under these conditions, the response functions are zero and the analysis described in the previous sections can be used to predict the ballistics of all three chambers. The angular location of the individual slots was calibrated by using the clockwise/counterclockwise rotation procedure developed for the single rotating valve.[8]

Figures 7 and 8 show the excellent agreement obtained between the predicted and observed amplitudes in all three chambers and in the phase angles between the various chambers. These phase angle data also show little difference

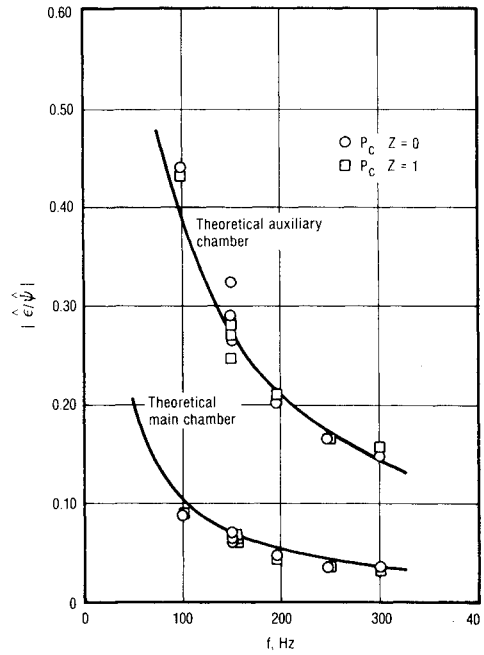

Fig.7 Amplitude from coldflow with blocked vent at $Z=0$.

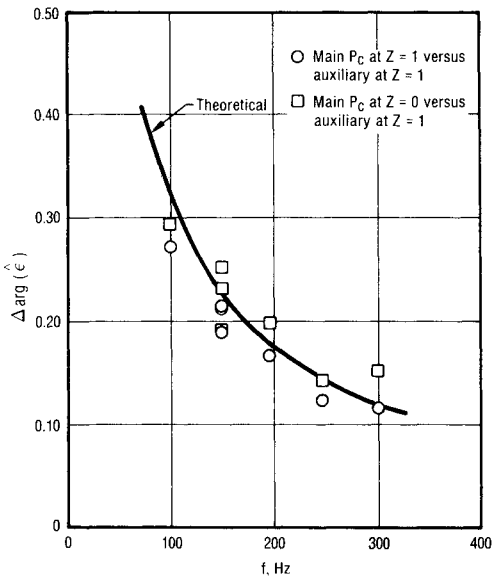

Fig. 8 Phase from coldflow with blocked vent at $Z=0$.

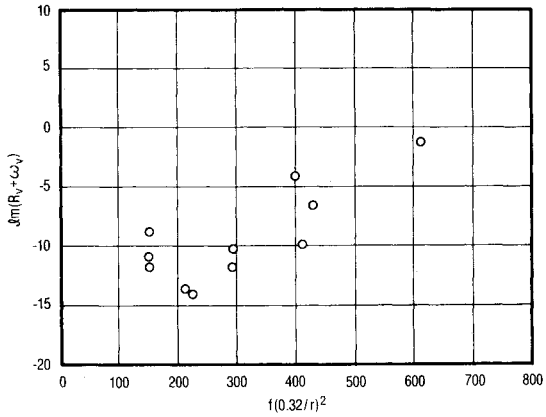

Fig. 9 Velocity-coupled response function derived from dual rotating valve data, UTP-19,933.

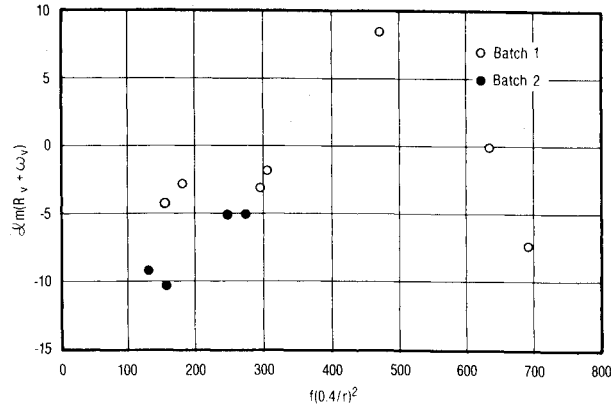

Fig. 10 Velocity-coupled response function derived from dual rotating valve data, UTP-19,942.

in the measurements made at each end of the combustion chamber. This substantiates the prediction that the burner operates as a bulk oscillation at low frequencies. This excellent agreement further substantiates the utility of the clockwise/counterclockwise method for calibrating the individual slot positions.

Combustion Tests

Combustion tests were then conducted to evaluate the apparatus and to measure velocity-coupled response functions using the standard rotating valve grains (7-cm-long by 2.5-cm-diameter initial port with a 0.64-cm web). Two nonaluminized formulations, UTP-19,933 and 19,942, were chosen because pressure-coupled response data were available.[27] More importantly, significant differences in the high-frequency combustion stability properties were observed in small motor tests. These two formulations, which differ only by the addition of 0.5% of a copper combustion modifier, have nearly identical (±10%) burning rates. Since high-frequency combustion stability involves gas phase processes, one could argue that perhaps these propellants would also have different velocity-coupled responses as well.

Figure 9 shows the imaginary part of the linear velocity response vs the thermal wave frequency parameter for UTP-19,933, the formulation that does not contain the additive. Some variations in propellant burning rate and combustion pressure were observed in these tests. This frequency parameter is one method for correcting for these variations. Cohen[28] has suggested a linear burning rate as a better method for normalizing these effects. Reference 25 contains a plot of these data using the Cohen approach, as well as a plot using the frequency directly. In all cases, the imaginary part of the linear velocity response was reported since this is the parameter used in stability predictions. As noted in the discussions on the analysis, no method has been developed for separating the nonlinear "response" from the threshold velocity.

These results show reasonable reproducibility from test to test, particularly when one considers the early state of development of this test method and the reproducibility difficulties in the velocity-coupled T-burner. Furthermore, the magnitude of the imaginary part is reasonable when compared to previously reported values obtained in the T-burner.[9,10] At first, one might consider the negative values to be suspicious at the lower frequencies, based on the thermal wave analogy to pressure-coupled response. T-burner data for nonaluminized propellants, however, have shown similar behavior, so these results are considered reasonable.

Figure 10 shows the results for UTP-19,942, the nonaluminized formulation containing the combustion modifier. Again, burning rate variations were noted between tests and these effects have been included in the frequency

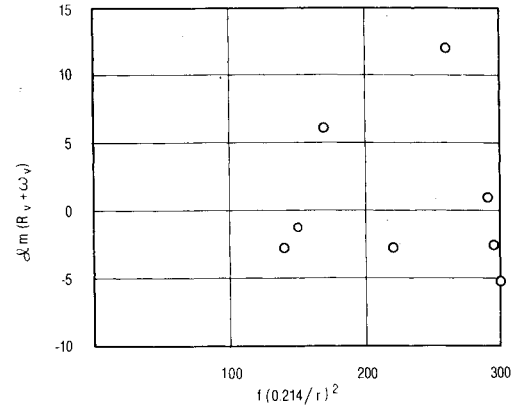

Fig. 11 Velocity-coupled response function derived from dual rotating valve data, UTP-19,360.

normalization. Reasonable reproducibility was again found between tests and between different batches of the same propellant, particularly if one accepts the frequency normalization and the possibility of multiple peaks in the response. More tests, however, particularly at frequencies between 400 and 600 Hz, are needed to establish these observations more conclusively.

Comparing the results for these two propellants shows significant differences in the magnitude of the imaginary part of the response. There are also important differences in the effect of frequency on the response. This suggests the test method can distinguish differences in propellant formulations and thereby might be useful for qualitatively ranking propellants. Comparisons between rotating valve and motor test results are needed, however, to establish this point conclusively.

Tests were also conducted with UTP-19,360, a low-burning-rate aluminized propellant, since this type of formulation is generally sensitive to erosive burning. Figure 11 shows the imaginary part of the response plotted against the normalized frequency. These results are more difficult to evaluate; one could conclude the scatter is excessive or that the response is characterized by multiple peaks. To clarify this point, the pressure response function data from the single rotating valve are shown in Fig. 12. If an analogy between pressure and velocity response can be made from thermal wave arguments, then one would conclude the velocity response exhibits considerable scatter.

Strand,[29] however, has also made pressure response function measurements on this propellant in the microwave bomb. His data suggest multiple peaks in the pressure response. (They also show a significant difference with the rotating valve data.) This would lead one to suggest the

velocity response should also show multiple peaks. Thus contradictory conclusions can be drawn by following this line of logic as well. This suggests that more work is required to resolve the question of reproducibility and multiple peaks for this aluminized propellant.

As noted earlier, the preceding results were interpreted using the linear velocity response model. Nonlinear velocity coupling is another possible framework for interpreting velocity response. This behavior would produce a high harmonic content in the oscillating pressures; hence data analyses were conducted to determine the harmonic content of the pressure oscillations. Amplitude frequency spectra, obtained from a test run at 600 Hz, are shown in Fig. 13. Several ensembles are shown simultaneously to demonstrate that the spectra are essentially constant during the entire test.

These data show significant harmonic content. Analysis of the area waveform[7] shows no driving of the even harmonics by the valve and only minimal (−25 dB) driving of the third harmonic. Thus the energy at the even harmonics is produced either by the combustion process or by the fluid mechanics of the burner, but not by the rotating valve drivers. Calculations were then made to determine if nonlinear acoustics or nonlinear velocity coupling could account for this harmonic content. The nonlinear acoustic calculations, described in detail in Ref. 25, predict the amplitude of the second harmonic is of the order of −55 dB of the fundamental component. Hence nonlinear acoustics could not generate these observed spectra.

On the other hand, the analysis indicates nonlinear velocity coupling could produce harmonic amplitudes of −25 dB compared to the fundamental. Thus these data suggest that nonlinear velocity coupling may be a better model to characterize the velocity response. Currently, the linear model is used to interpret laboratory data and to predict motor stability. This could be the wrong approach. Hence this observation warrants substantial additional study since selection of the proper model can have a significant influence on stability predictions in motors.

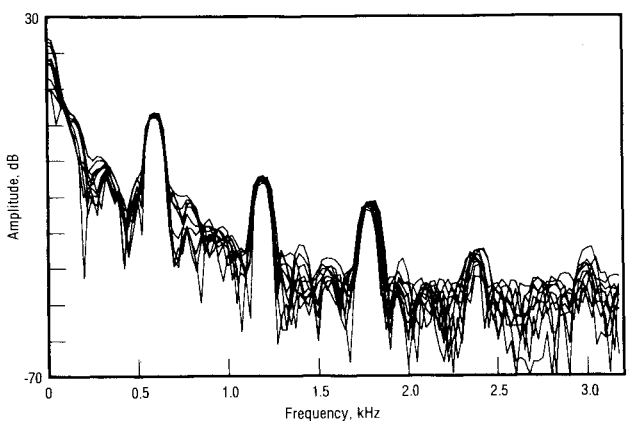

Fig. 12 Pressure response data, UTP-19,360.

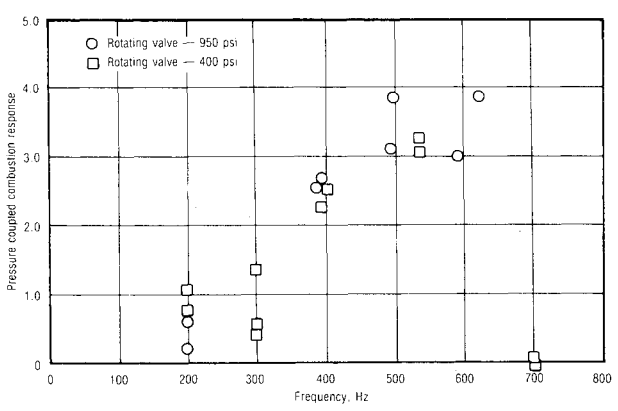

Fig. 13 Frequency spectra during test.

Conclusions

The dual rotating valve approach shows good promise as a method for measuring velocity-coupled response functions of solid propellants. Reasonable reproducibility has been demonstrated and the magnitude of the response is consistent with results from alternative methods. To be fully accepted, however, more thorough comparison with predicted values or results from alternative methods, is required. Unfortunately, suitable predictive methods are not available and alternative methods are subject to substantial uncertainties. Hence the validity of data from this method for motor stability predictions is uncertain.

A further complication is the lack of evidence to establish the validity of either of the two conceptual models for velocity coupling. Data from the dual rotating valve have a high harmonic content, which suggests a nonlinear model may be more appropriate. This is also consistent with results from the various T-burner studies on this subject. However, this is not sufficient evidence to separate these models. Hence basic analyses and experiments are required to define the fundamental coupling mechanisms. Once defined, all the laboratory test methods can be examined and their relevance to motor conditions evaluated.

Acknowledgments

The authors wish to thank P.G. Willoughby for his many helpful suggestions and for his detailed design of the experimental apparatus. This work was supported by the Air Force Office of Scientific Research under Contract F49620-77-C-0048.

References

[1] Brown, R.S. and Muzzy, R.J., "Linear and Nonlinear Pressure Coupled Combustion Instability of Solid Propellants," *AIAA Journal,* Vol. 8, Aug. 1970, pp. 1492-1500.

[2] Culick, F.E.C., "A Review of Calculations for Unstable Burning of a Solid Propellant," *AIAA Journal,* Vol. 6, Dec. 1968, pp. 2241-2254.

[3] Lengelle, G., "A Model Describing the Velocity Response of Composite Propellants," *AIAA Journal,* Vol. 13, March 1975, pp. 315-322.

[4] Friedly, J.C. and Petersen, E.E., "Influence of Combustion Parameters on Instability at Solid Propellant Motors, Part II, Nonlinear Analysis," *AIAA Journal,* Vol. 4, Nov. 1966, pp. 1932-1937.

[5] Condon, J.A., "A Model for the Velocity Coupled Response of Composite Propellants," Paper presented at 16th JANNAF Combustion Conference, Monterey, Calif., Sept. 1979.

[6] Brown, R.S., Culick, F.E.C., and Zinn, B.T., "Experimental Methods for Combustion Admittance Measurements," *Progress in Astronautics and Aeronautics,* Vol. 63, 1978, pp. 191-120.

[7] Brown, R.S., Erickson, J.E., and Babcock, W.R., "Combustion Response Function Measurements by the Rotating Valve Method," *AIAA Journal,* Vol. 12, Nov. 1974, pp. 1502-1510.

[8] Brown, R.S., "Development and Evaluation of Rotating Valve Combustion Response Test Techniques," AFRPL-TR-75-72, Oct. 1976.

[9] Beckstead, M.W. and Butcher, A.G., "The Velocity Coupled T-Burner," AIAA Paper 74-200, AIAA, 1974.

[10] Micheli, P.L., "Investigation of Velocity Coupled Combustion Instability," AFRPL TR-76-100, 1977.

[11] Beckstead, M.W., "Velocity Coupling Workshop," Paper presented at the 16th JANNAF Combustion Conference, Monterey, Calif., Sept. 1979.

[12] Eisel, J.L. and Dehority, G.L., "A Technique for Investigating Low Frequency Velocity-Coupled Combustion Instability," CPIA Pub. No. 105, Vol. 1, pp. 703-712.

[13] Price, E.W. and Dehority, G.L., "Velocity Coupled Axial Mode Combustion Instability in Solid Propellant Rocket Motors," Paper presented at the ICRPG/AIAA 2nd Solid Propulsion Conference, Anaheim, Calif., June 1967, pp. 213-227.

[14] Dehority, G.L. and Price, E.W., "Axial Mode, Intermediate Frequency Combustion Instability in Solid Propellant Rockets," Naval Weapons Center Rept. NWC-TP-5654, Oct. 1974.

[15] Culick, F.E.C., "Stability of Longitudinal Oscillations with Pressure and Velocity Coupling in a Solid Propellant Rocket," *Combustion Science and Technology,* Vol. 2, No. 4, 1970, pp. 179-201.

[16] Kruse, R.B. and Glick, R.L., "Velocity-Coupled Instability in Prototype RS MK 36 Motors," Paper presented at 16th JANNAF Combustion Conferene, Monterey, Calif., Sept. 1979.

[17] Mathes, H.B., "Assessment of Chamber Pressure Oscillations in Shuttle SRB," Paper presented at 16th JANNAF Combustion Conference, Monterey, Calif., Sept. 1979.

[18] Beddini, R.A., "A Reacting Turbulent Boundary Layer Approach to Solid Propellant Erosive Burning," *AIAA Journal,* Vol. 16, Sept. 1978, pp. 898-905.

[19] Zucrow, M.J., Osborn, J.R., and Murphy, J.M., "An Experimental Investigation of the Erosive Burning Characteristics of a Nonhomogeneous Solid Propellant," AIAA Paper 64-107, 1964.

[20] Lovine, R.L., Dudley, D.P., and Waugh, R.C., "Standardized Stability Prediction Method for Solid Rocket Motors," AFRPL-TR-76-32, May 1976.

[21] Culick, F.E.C., "The Stability of One Dimensional Motions in a Rocket Motor," *Combustion Science and Technology,* Vol. 7, No. 4, 1973, pp. 165-175.

[22] Murphy, G.M., *Ordinary Differential Equations and Their Solutions,* Van Nostrand Reinhold Company, New York, 1960, p. 323.

[23] Abramowitz, M. and Stegan, I.A., "Handbook of Mathematical Functions with Formulas, Graphs, and Mathematical Tables," National Bureau of Standards Applied Mathematics Series No. 55, 1964.

[24] Micci, M.M., Caveny, L.H., and Sirignano, W.A., "Linear Analysis of Forced Longitudinal Waves in Rocket Motor Chambers," *AIAA Journal,* Vol. 19, Feb. 1981, pp. 198-204.

[25] Brown, R.S. and Waugh, R.C., "Rotating Valve for Velocity Coupled Combustion Response Measurements," AFOSR-TR-80-0055, Nov. 1979.

[26] Hewes, J.C., private communication, 1977.

[27] Rudy, T.P., Bain, L.S., and Newman, B.D., "Chemical Control of Propellant Combustion" AFRPL-TR-78-15, April 1978.

[28] Cohen, N.S., Taylor, D.E., Small, K.R., Epstein, R.H., and Churchill, H.L., "Design of a Smokeless Solid Rocket Motor Emphasizing Combustion Stability," CPIA Pub. No. 27, Vol. 2, pp. 205-220.

[29] Strand, L.D., private communication, 1979.